Optical Molecular Imaging in the Gastrointestinal Tract

Jennifer Carns[1a#], PhD, Pelham Keahey[1b], BS, Timothy Quang[1c], BS,

Sharmila Anandasabapathy[2d], MD, Rebecca Richards-Kortum[1e*], PhD

* corresponding author after publication

corresponding author for proofs

1. Department of Bioengineering, Rice University, Houston, TX 77005, United States

a. jcarns@rice.edu, b. keaheyp@gmail.com, c. tquang03@gmail.com,

d. sharmila.anandasabapathy@mountsinai.org e*. rkortum@rice.edu

2. Division of Gastroenterology, Mount Sinai Medical Center, New York, NY 10029, United States

Abstract:

Recent developments in optical molecular imaging allow for real-time identification of morphological and biochemical changes in tissue associated with gastrointestinal neoplasia. This review summarizes widefield and high resolution imaging modalities currently in pre-clinical and clinical evaluation for the detection of colorectal cancer and esophageal cancer. Widefield techniques discussed include high definition white light endoscopy, narrow band imaging, autofluoresence imaging, and chromoendoscopy; high resolution techniques discussed include probe-based confocal laser endomicroscopy, high-resolution microendoscopy, and optical coherence tomography. Finally, new approaches to enhance image contrast using vital dyes and molecular-specific targeted contrast agents are evaluated.

Introduction

Gastrointestinal (GI) neoplasia is a leading contributor to global cancer mortality and morbidity [1]. Early detection of cancers of the gastro-intestinal tract significantly improves patient outcomes; however, current clinical practice often fails to detect these cancers until they are at an advanced stage when treatment is more invasive, more expensive, and less successful [1-3]1. This review highlights the potential of new optical molecular imaging techniques to improve early detection of GI cancers, with a focus on two important sites: colorectal cancer and esophageal cancer.

Colorectal cancer is a leading cause of cancer related deaths worldwide [1]. In the United States, it is the third most common cancer amongst men and women and accounts for 9% of all cancer deaths. The 5-year survival rate increases from 64% to 90% when detection occurs during the early stages of development [4]. Since the prognosis of late stage colorectal cancer is so poor, it is important to accurately screen patients. Colorectal cancer can be prevented by the removal of colorectal polyps before they progress to cancer. Although colonoscopy is highly sensitive and has the potential to prevent approximately 65% of colorectal cancers from developing, some polyps can still be missed, prompting the need for increasingly sensitive imaging techniques [5,6].

The incidence of esophageal adenocarcinoma (EAC) is rapidly increasing worldwide. Approximately 24,000 cases of EAC are diagnosed each year in the United States. The 5-year survival rate for late stage EAC is only 2.8%, whereas for local-staged tumors it is 49.3% [4]. With earlier diagnosis, however, the 5-year survival rate for stage 0 EAC exceeds 95% [7]. Barrett's esophagus (BE) is a benign treatable condition of the esophagus that arises due to acid

reflux. Individuals with BE are at higher risk of developing precancerous lesions, which can progress to EAC. Because of this increased risk, it is recommended that individuals with BE undergo routine endoscopic examination at regular intervals to facilitate detection and treatment of precancers and early cancers. However, using standard, white light endoscopy it can be difficult to identify early neoplastic lesions. Thus, routine endoscopic surveillance of BE also includes random four-quadrant biopsies taken every 1-2 cm along the Barrett's segment [3,4]. Studies have shown that random four-quadrant biopsies can have miss rates up to 48% [8,9]. Furthermore, random four-quadrant biopsies taken every 2 cm can miss up to half of the cancers found when a protocol of 1 cm is used [10].

Thus, there is an important need for new approaches that can improve the ability to identify early neoplastic lesions in the GI tract. This need has prompted the development of new optical imaging modalities to improve recognition and enable *in vivo* characterization of suspicious lesions in the GI tract. These approaches leverage both endogenous optical contrast as well as the use of contrast agents targeted against biomarkers that are associated with early neoplasia. This review summarizes recent advances in optical molecular imaging techniques to recognize early neoplastic disease in the GI tract. The paper first discusses new approaches that are in clinical evaluation; these approaches are based primarily on endogenous optical contrast and/or the use of vital dyes to enhance image contrast. The paper then describes approaches in development and preclinical evaluation, including the development of molecular-specific targeted contrast agents.

Clinical Studies

Several complementary widefield and high resolution imaging techniques are being evaluated to assist in the endoscopic detection and characterization of early neoplasia in the GI tract. Wide-field imaging modalities are designed to survey large areas of tissue, while high resolution imaging is limited to smaller fields of view but can achieve subcellular resolution. A variety of studies have been conducted to evaluate the performance of widefield imaging and high resolution imaging techniques in the clinical setting. An overview of these emerging technologies and the results of several recent clinical studies are provided in this section.

Widefield Imaging

With the development of high definition white light endoscopy (HD-WLE), the spatial resolution of standard white light endoscopy (WLE) has been drastically improved [11]. Narrow band imaging (NBI) is a complementary widefield technique that can assist in tissue characterization by enhancing the visibility of vasculature in the tissue via illumination with narrow bands of blue and green light, selected to match spectral regions with increased hemoglobin absorbance [12]. Neoplastic changes are often accompanied by an increase in microvasculature density. Hemoglobin is known to absorb wavelengths between 400-500 nm. The visualization of microvasculature can therefore be enhanced by using optical filters to only pass two bands of illumination. Generally, green (530-550 nm) and blue (390-445 nm) wavelengths are used. The absorption of blue and green light by hemoglobin causes the vasculature to appear much darker than surrounding tissue without the need of a contrast agent.

Several clinical studies have been conducted to assess the effectiveness of NBI for detecting early neoplasia, but they have produced varying results. Some recent studies performed with the Olympus GIFQ240 have shown advantages of NBI as compared to HD-WLE

[13,14]. In a single center study involving 75 cites on 21 patients with BE, Singh *et al*. compared diagnoses made with NBI and HD-WLE to histology results and found that the NBI diagnosis agreed with the histology results more often than HD-WLE (88.9% vs. 71.9%) [13]. Muto *et al*. conducted a multicenter randomized trial comparing the detection rates of NBI and HD-WLE for early superficial esophageal squamous cell carcinoma (ESCC), a condition unrelated to BE. Of the 121 patients with histologically confirmed superficial ESCC, 63 patients with a total of 107 lesions were evaluated primarily with NBI followed by a secondary evaluation with HD-WLE, and the remaining 58 patients with a total of 105 lesions were evaluated primarily with HD-WLE followed by NBI. In the first group NBI alone detected 104 of the 107 lesions, while in the second group HD-WLE alone detected only 58 of the 105 lesions, yielding sensitivities of 97% and 55%, respectively. However, when the results of the secondary evaluations were considered, HD-WLE did not find any additional lesions in the first group, but the addition of NBI with HD-WLE in the second group increased the sensitivity to 95% [14].

However, other recent studies performed with the Olympus H180 have indicated that the performance of NBI and HD-WLE are similar [15,16]. Sharma *et al*. investigated the detection rate of intestinal metaplasia (IM) and neoplasia, the detection rate of neoplasia specifically, and the number of overall biopsies performed in 123 patients with BE for evaluations with NBI and HD-WLE. Half of the patients were randomly selected to receive HD-WLE examination, where biopsies of visible lesions were taken followed by random four quadrant biopsies for every 2 cm of the BE segment. The remaining patients received NBI examination, where biopsies were first taken of visible lesions, followed by targeted biopsies of areas detected by NBI. All patients returned within 3-8 weeks to receive the alternative procedure from a different endoscopist. Both modalities identified 104 of 113 patients with intestinal metaplasia, demonstrating a

detection rate of 92%. Patients that were missed by the first procedure were found to have IM in the subsequent procedure. NBI resulted in a total of 267 biopsies, while the standard 2 cm protocol resulted in 321 biopsies with HD-WLE. Histology was used to classify each biopsy as no IM, IM, low-grade dysplasia (LGD), high-grade dysplasia (HGD), or EAC. NBI did detect significantly more areas for any form of neoplasia, but when the analysis was limited to areas with HGD or EAC, there was no statistical difference between the two modalities. However, NBI did require fewer biopsies per patient (3.6 vs. 7.6, respectively) [16]. Pasha *et al.* analyzed a series of randomized controlled trials to determine the detection rate and miss rate for colon polyps and adenomas by NBI and HD-WLE. They evaluated six studies for the detection of adenomas and the detection of patients with polyps, four studies for the detection of patients with adenomas, and five studies for the detection of adenomas <10 mm, flat adenomas, and the number of flat adenomas per patient, and found no statistical difference in the performance of NBI and HD-WLE. They also found no statistical difference in the polyp miss rate (three studies) or adenoma miss rate (three studies) between the two modalities [17].

Another widefield imaging technique, autofluorescence imaging (AFI), uses one wavelength of light to stimulate endogenous fluorophores in the tissue, triggering the emission of fluorescent light at longer wavelengths. The emitted light can be imaged on a charge-coupled device (CCD) using an emission filter to block scattered excitation light. Neoplasia is associated with changes in endogenous fluorescence; neoplastic epithelial cells are associated with increased fluorescence from mitochondrial co-factors NAD(P)H and FAD and collagen in the stroma near neoplastic lesions shows reduced fluorescence [18]. Like NBI, AFI does not require the application of a contrast agent. While studies have shown that AFI results in an increase in sensitivity for detection of early neoplasia in BE as compared to WLE, it has also

demonstrated high false positive rates [19-23]. False positive rates as high as 40% have been reported using AFI for detection of early neoplasia in BE [19]. The high false positive rate of AFI is attributed to inflammation, which is also associated with loss of auto-fluorescence [20, 21] . Studies have indicated that when NBI is used in combination with AFI the false positive rate can be reduced, but in these studies NBI has misidentified high grade dysplasia as normal [19, 22].

A recent study by Curvers *et al*. compared the performance of the endoscopic trimodal imaging (ETMI) system (Olympus GIFQ260FZ, available in Europe and Asia) to standard WLE. The ETMI system can perform HD-WLE, AFI, and NBI. The study compared the detection rate of early neoplasia in Barrett's esophagus for each modality in 99 patients with low-grade intraepithelial neoplasia. All of the patients underwent two consecutive procedures with the ETMI (consisting of HD-WLE followed by AFI and NBI) and standard WLE in random order, each performed by two separate endoscopists with no particular expertise in BE or advanced imaging techniques. The endoscopist performing the second procedure was blinded to the results of the first procedure. Targeted biopsies were first taken from areas identified as suspicious, and the imaging modality that detected each suspicious area was noted. Four quadrant random biopsies every 2 cm were then taken. In Figure 1A through 1C, images from a patient with no lesions are shown for HD-WLE, AFI, and WLE, respectively. In Figure 1D and 1E, an early carcinoma is observed with HD-WLE and WLE, respectively. An additional lesion is visible via AFI, indicated by the yellow arrow in Figure 1G, which was not visible in the HD-WLE image of Figure 1F. The NBI image of Figure 1H shows suspicious abnormal blood vessels in the area of the lesion. This study found no significant difference in the overall (targeted + random) detection of dysplasia by ETMI versus standard WLE. There was no significant difference in the

targeted detection of dysplastic lesions (low-grade intraepithelial neoplasia, high-grade intraepithelial neoplasia, or carcinoma) with HD-WLE detecting dysplasia in 23 patients as compared to 21 patients with standard WLE. However, the addition of AFI led to the detection of an additional 22 dysplastic lesions in 14 patients, increasing the number of detected patients from 21 to 35. NBI was associated with a decrease in the false positive rate, but was also associated with a reduction in sensitivity. Of the 24 patients with high grade intraepithelial neoplasia or carcinoma, random biopsies led to detection in only 6 patients evaluated with ETMI and 7 patients evaluated with standard WLE [23].

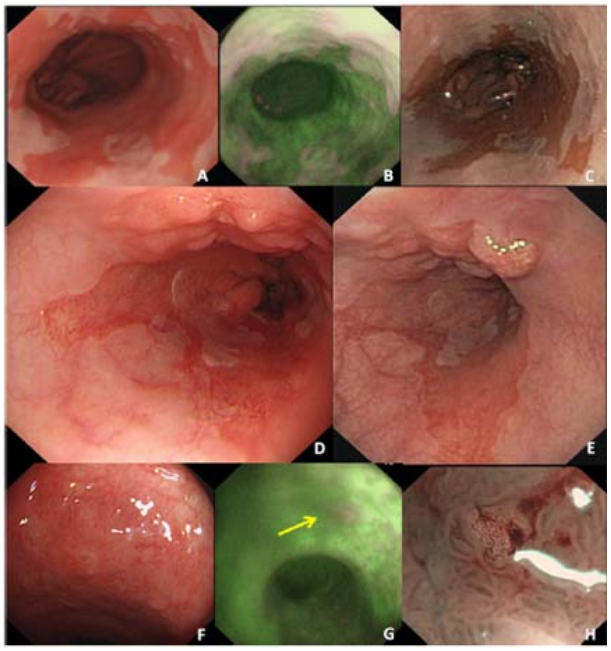

Figure 1. Top row: widefield images acquired from endoscopically normal esophagus with (A) HD-WLE, (B) AFI, and (C) standard WLE. Middle row: widefield images acquired from an early carcinoma with (D) HD-WLE and (E) WLE; the carcinoma is located at the 12 o'clock position. Bottom row: (F) and (G) show an AFI positive lesion (arrow) containing high-grade intra-epithelial neoplasia that was not seen during HD-WLE. (H) NBI showed irregular mucosal and vascular patterns and abnormal blood vessels suspicious for dysplasia. (Curvers W, van Vilsteren FG, Baak LC, *et al.* Endoscopic trimodal imaging versus standard video endoscopy for detection of early Barrett's neoplasia: a multicenter randomized, crossover study in general practice. Gastrointest Endosc 2011;73:195-203; with permission)

Other widefield imaging techniques have exploited contrast agents to enhance the visibility of neoplastic changes. Chromoendoscopy involves the use of stains, such as Lugol's iodine, to differentiate the areas of stratified squamous epithelium from areas of metaplasia associated with BE [12]. Ishimura *et al.* investigated the use of NBI and chromoendoscopy to assist in the detection of squamous islands for the diagnosis of short-segment BE, which is

characterized by segments of metaplasia that are less than 2–3 cm in length. The number of identifiable squamous islands was documented first with HD-WLE, followed by NBI, and finally with chromoendoscopy, as shown in Figure 2A through 2C, respectively. Of the 100 patients evaluated in the study, squamous islands were visible in 48 of the patients using HD-WLE, 71 patients with NBI, and 75 patients with chromoendoscopy. NBI exhibited a detection rate of 94.7% as compared to chromoendoscopy. By contrast, HD-WLE demonstrated a detection rate of 64% when compared to chromoendoscopy. The mean number of detected squamous islands for HD-WLE, NBI, and chromoendoscopy was 0.55 ± 0.06, 1.02 ± 0.09, and 1.76 ± 0.18, respectively. While chromoendoscopy remains the most accurate way of visibly identifying squamous islands, NBI yielded comparable results without the risk of side effects from the use of Lugol's iodine [24].

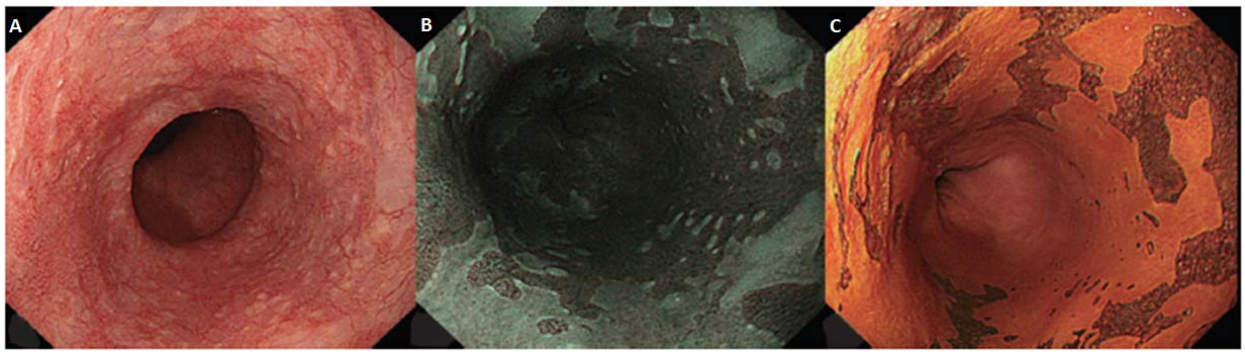

Figure 2. Endoscopic identification of the squamous islands in short-segment Barrett's esophagus with three different modalities: white light endoscopy (a), narrow band imaging endoscopy (b), and iodine chromoendoscopy (c). (Ishimura N, Amano Y, Uno G, et al. Endoscopic characteristics of short-segment Barrett's esophagus, focusing on squamous islands and mucosal folds. J Gastroenterol Hepatol 2012;27:82-7; with permission)

High Resolution Imaging

High resolution imaging modalities can achieve sub-cellular resolution, albeit with small fields of view. This approach, which can provide an image similar to what is seen in histology, is often termed "optical biopsy". High resolution imaging is especially useful for targeting biopsies by providing a live image of the cellular architecture before the biopsy is taken [25-28]. There are a number of different high resolution imaging modalities currently being used *in vivo;* these include confocal laser endomicroscopy (CLE) [24-27] and high resolution microendoscopy [34, 35].

The main advantage of CLE over conventional microscopy is the use of a spatial filter to reject out-of-focus light, capturing preferentially from tissue located at the focal point of the imaging system. Because only the light from the focal plane of the system is captured, images can also be acquired at different depths. The typical resolution achievable with CLE is on the order of 1-2 microns with a field of view of approximately 500-700 μm^2. CLE can be used either to image reflected light, or to image fluorescent light, typically with exogenous fluorescent contrast agents, such as fluorescein, acraflavine, and proflavine [24-26,29,31,32]

In practice, there are several variations of CLE that are used to acquire high resolution images. A commonly used type of CLE is probe-based confocal laser endomicroscopy (pCLE). pCLE employs a coherent optical fiber bundle composed of over 10,000 optical fibers as the conduit between the light source and the tissue. Since only the remitted light originating from the focal point will propagate back through the fiber bundle efficiently, each individual fiber acts as a spatial filter to reject the out-of-focus light, providing optical sectioning. By scanning the excitation light across the entire bundle, a high resolution image can be formed. Commercial

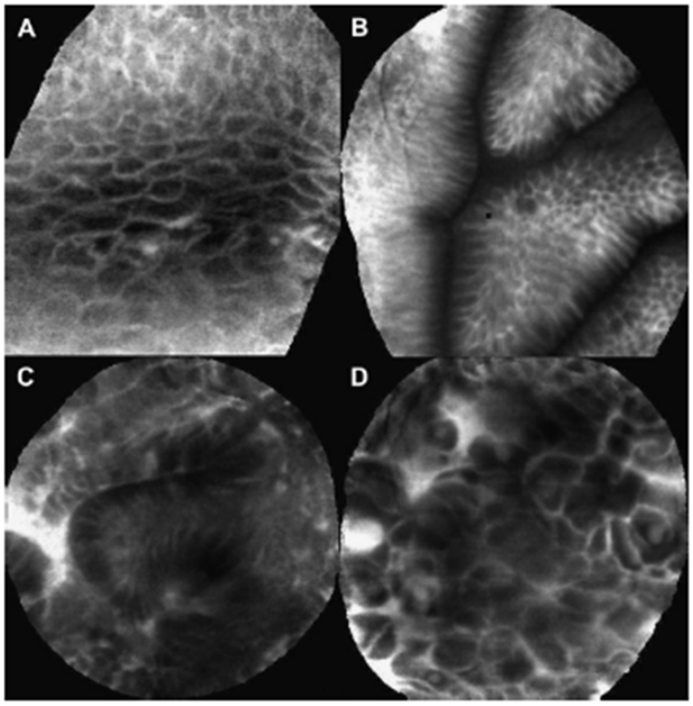

Figure 3. pCLE imaging of normal squamous epithelium in the esophagus (A), BE without dyslplasia (B), high-grade dysplasia (C), and carcinoma (D). (Shahid MW and Wallace MB. Endoscopic Imaging for the Detection of Esophageal Dysplasia and Carcinoma. Gastrointest Endosc Clin N Am 2010;20:11-24; with permission)

systems from companies such as Mauna Kea Technologies (CellVizio) and Pentax are available and have been used in several studies [25-27,30,31]. Figure 3 shows representative fluorescence images of 4 distinct sites of normal squamous epithelium in the esophagus, Barrett's esophagus, high grade dysplasia, and squamous cell carcinoma [32]. Fluorescein was the contrast agent used to acquire these images. The variations in tissue architecture between the different sites can be clearly visualized.

Several studies have compared the performance of confocal microendoscopy to HD-WLE examination and narrow-band imaging in the esophagus and colon. Sharma *et al.* assessed the sensitivity and specificity of pCLE in conjunction with HD-WLE compared to HD-WLE alone in a prospective, randomized, multi-center trial including 101 patients with BE. Images were acquired in fluorescence mode with fluorescein (2.5 mL, 10%) as the contrast agent. After each site was imaged with pCLE, a biopsy was taken at the same location for histopatholgical assessment. The sensitivity and specificity were reported to be 34.2% and 92.7% respectively for HD-WLE alone and 68.3% and 87.8% for HD-WLE with pCLE. Out of the 120 sites

diagnosed with high grade dysplasia or early carcinoma, HD-WLE alone missed 79 sites while the addition of pCLE reduced the number of missed sites to 38 [26].

Wang *et al.* also employed pCLE to image the colon *in vivo* in a study of 54 patients. Fluorescence images were acquired following the administration of fluorescein. After imaging, a pinch biopsy was also acquired at each site for histopathology. Image analysis was performed in this study to distinguish between normal mucosa, hyperplasia, tubular adenoma, and villous adenoma. Analysis of each image consisted of calculating the fluorescence contrast ratio which was defined as the ratio of the mean intensity of the lamina propria to the mean intensity of a crypt in a selected region of interest. Using the fluorescence contrast ratio, the study documented a sensitivity and specificity of 91% and 87%, respectively, when distinguishing between normal and lesional mucosa (including hyperplasia and adenomatous lesions). In addition, high sensitivities and specificities were found when distinguishing hyperplasia from adenoma (97% and 96%) and tubular adenoma from villous adenoma (100% and 92%) [31].

Another use for high-resolution imaging is detecting neoplasia after therapy. Endoscopic mucosal resection (EMR) is generally considered appropriate for flat neoplastic lesions less than 1.5 cm in size that can be easily accessed by the endoscope [33]. High resolution imaging techniques can be useful in determining the perimeters for EMR, ensuring that all neoplastic areas have been removed. Shahid *et al.* evaluated the diagnostic accuracy of pCLE in detecting residual colorectal neoplasia after EMR in a prospective blind study of 92 patients. The goal was to compare pCLE to chromoendoscopy techniques such as NBI and to assess the diagnostic accuracy of the two modalities used together. Fluorescein was used as a contrast agent when performing pCLE. In the study, 92 patients had EMR's performed on a total of 129 sites. The EMR scars were imaged at all 129 sites. Histology determined that 29 sites had residual

neoplasia. NBI was able to identify the residual neoplasias with a sensitivity and specificity of 72% and 78%, respectively while pCLE was reported to have sensitivity and specificity of 97% and 77%. When the two modalities were combined, a sensitivity and specificity of 100% and 87% was reported [25].

High-resolution microendoscopy (HRME) is another fiber bundle based confocal technology that offers a portable, low-cost alternative to traditional confocal microendoscopy [34, 35]. Similar to pCLE, HRME acquires images by placing the fiber bundle in direct contact with the tissue surface. Instead of scanning through each optical fiber as with pCLE, each fiber in the bundle acts as an individual pixel which collectively forms a high resolution image that is comparable with other confocal microendoscopy techniques. HRME has been evaluated for use in a few studies for the GI tract [34, 35]. Additionally, it has been evaluated in a preliminary study in northern China. In this study, the performance of HRME was compared to the performance of chromoendoscopy using Lugol's iodine. Preliminary results have shown that even novice users can be trained to differentiate between normal, dysplastic, and neoplastic tissues with the HRME (http://www.youtube.com/watch?v=eJi28REXN_M).

Preclinical Development

In the preclinical setting, many groups are working to develop new contrast agents, including both vital dyes and molecular-targeted agents, to enhance widefield and high resolution imaging. Also, as imaging techniques have matured, there has been an increased focus on the co-registration of widefield molecular imaging and high resolution imaging. Some recent developments are highlighted below.

Widefield Imaging

While proflavine, a vital dye, has been primarily used clinically as a contrast agent to assist in high resolution imaging studies, Thekkek *et al.* recently demonstrated proflavine for use in widefield fluorescence imaging. Proflavine was applied to resected specimens from patients who underwent an EMR, esophagectomy, or colectomy. The contrast agent enhanced visualization of glandular structure in widefield fluorescence images, including glandular distortion and effacement in Barrett's-associated neoplasia, as well as irregularly spaced colonic crypts associated with colonic dysplasia during fluorescence imaging [21].

Bird-Lieberman *et al*. studied the use of lectins as a molecular-targeted agent to identify progression of Barrett's esophagus to carcinoma *ex vivo*. They examined gene expression profiling data from samples at various stages of progression and determined that upregulation of cell-surface glycan degradation pathways corresponded with progression from Barrett's to EAC. Accordingly, lectins such as wheat germ agglutinin (WGA), helix pomatia agglutinin (HPA), and aspergillusoryzae lectin (AOL) all exhibited reductions in binding to the human esophagus during EAC progression. Histochemical analysis subsequently showed that WGA and AOL had the most significant reduction in binding with progression of Barrett's to EAC. WGA was chosen for further study as a molecular probe due to its common presence in human diets. WGA labeled with fluorescein was applied to resected esophagi *ex vivo* and imaged using widefield techniques. Both white light imaging and AFI performed without the WGA-fluorescein contrast agent identified no abnormalities. However, after the application of WGA areas of reduced fluorescence were observed correlating to areas of reduced WGA binding and dysplasia, as shown in Figure 4. The WGA contrast agent was able identify areas of dysplasia that would have otherwise been missed with normal WLE and AFI [36].

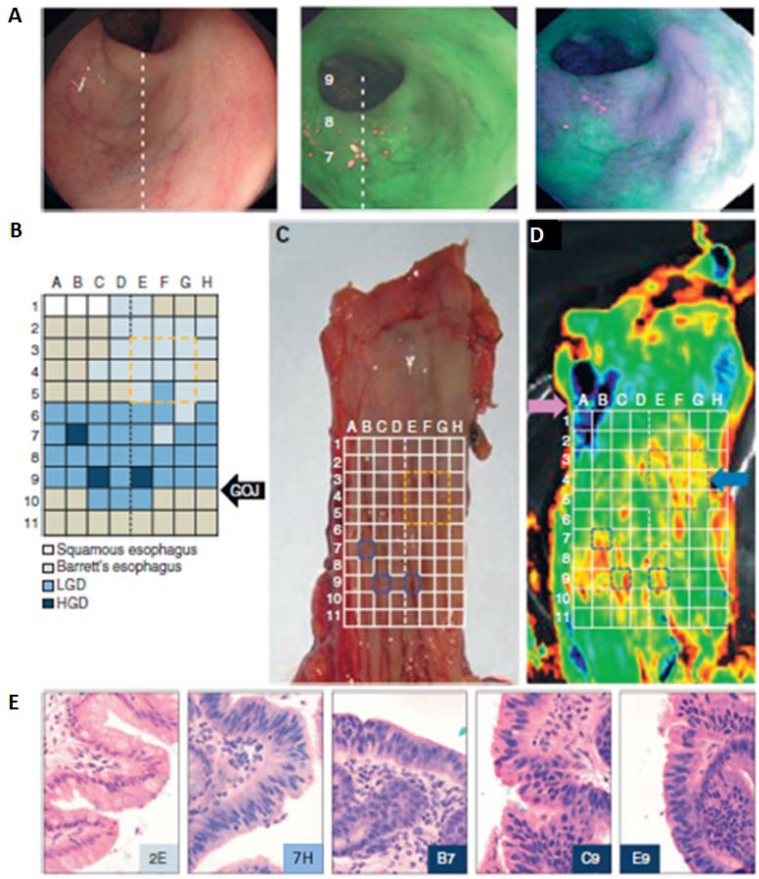

Figure 4. Whole-organ imaging *ex vivo*.(a) White-light (left), fluorescence at 490–560 nm prior to the application of WGA (middle), fluorescence at 490–560 nm after application of WGA and Alexa Fluor 488 (right). Areas of low WGA binding appear in purple and high binding in green. The dashed white line is to facilitate orientation between images. (b) Grid showing pathological map of the resected specimen. The black dashed line in b represents the longitudinal axis shown in a. (c) The same specimen opened longitudinally with grid overlay from b. (d) Esophagus specimen imaged using an IVIS 200 camera which quantified fluorescence by color coded map. The pink arrow marks an area of artifact from the exposed submucosal tissue, and the blue arrow indicates the site of a previous endoscopic mucosal resection (outlined with a dashed gray box). (e) Histology from various grid locations. (Bird-Lieberman EL, Neves AA, Lao-Sirieix P, *et al*. Molecular imaging using fluorescent lectins permits rapid endoscopic identification of dysplasia in Barrett's esophagus. Nat Med 2012;18:315-21; with permission)

In an *in vivo CPC;Apc* mouse model study Miller *et al*. developed a fiber optic multispectral scanning endoscope designed to image multiple molecular targets simultaneously for use in early diagnosis of colorectal cancer. They identified three peptides (KCCFPAQ, AKPGYLS, LTTHYKL) that exhibited specific binding to colorectal adenomas and labeled them using fluorescence labels with minimal spectral overlap. Images acquired with the multispectral endoscope could be used to differentiate the emission spectra of two of these labels successfully, enabling simultaneous imaging of two molecular probes *in vivo*. Spatially distinguishable binding patterns were apparent during imaging, suggesting different binding targets for the peptides in dysplastic tissue. However, the author indicates that further study into

distinguishable dyes for molecular agents and algorithms to account for variations in tissue morphology and orientation are needed [37].

High resolution imaging: increasing accuracy

One of the key limitations of high resolution imaging is the limited field of view. Consequently, high resolution techniques sample only a small fraction of the mucosal surface at risk, presenting challenges especially in heterogeneous regions of tissue. Two techniques have been evaluated to overcome this limitation. One option is to couple the use of high resolution imaging with a widefield imaging system, employing the widefield system first to identify areas of suspicion, which can then be characterized by a high resolution system. Another technique recently developed is video mosaicing, in which consecutive video frames acquired with a high resolution system are stitched together as the probe is advanced along the tissue. This is can be especially useful for visualizing the extent of a lesion and giving a broader sense of the overall tissue morphology. Video mosaicing can allow a clinician to acquire high resolution images from areas approximately 2 – 30x larger than one single field of view [38,39]. While video mosaicing is a promising approach, current publications have only demonstrated its use in post-processing.

There has also been a focus on developing targeted contrast agents to be used with high resolution imaging. Goetz *et al*. used fluorescently labeled EGFR antibodies as a contrast agent for detection of colorectal cancer. Confocal laser endomicroscopy images were acquired from mice *in vivo* (n = 68) in addition to *ex vivo* specimens of human colorectal mucosa. Tumors in the mice were established using human colorectal cancer cell lines with high (SW480) or low

(SW620) expression of EGFR. In the rodent model, the confocal probe was scanned across the surface of the tumor to acquire fluorescence images. The tumors were also processed for histology and immunohistochemistry. Images acquired from the mice *in vivo* were graded on a 0-3+ scale by two independent investigators according to fluorescence intensity of each image. Mice with a tumor containing the SW480 line were found to have significantly higher mean fluorescence intensity (1.92 ± 0.22) than mice with SW620 tumors (0.59 ± 0.21). The resected, *ex vivo* human colorectal mucosa specimens were incubated with antibody solution and also imaged. There was a statistically significant difference in the mean fluorescence intensity for neoplasia (2.13 ± 0.30) and normal mucosa (0.25 ± 0.16) [29].

In an *in vivo* human trial, Hsiung *et al*. has demonstrated the use of a specific contrast agent that targets colonic dysplasia with pCLE. The contrast agent used was a fluorescently labeled heptapeptide sequence which was determined to specifically bind to areas of colonic dysplasia. In this study, polyps were first endoscopically identified. Following identification, the peptide was applied and then imaged with pCLE. A neighboring, normal region of mucosa was also imaged. Polyps imaged with pCLE were then biopsied and processed for histology. Characteristic fluorescence images of the colon are displayed in Figure 5. As can be seen, the contrast agent primarily binds to the dysplastic crypts, while the normal crypts are unlabeled. A total of 18 polyps were imaged with 5 representative images selected for each polyp. Analysis of the acquired images consisted of comparison of the mean fluorescence intensity between normal mucosa and the adenoma in three 25 x 25 μm regions of interest for each image acquired, yielding a total of 270 different regions of interest. This resulted in a sensitivity and specificity of 81% and 82%, respectively, when comparing the mean fluorescence intensity between normal tissue and adenomas [40].

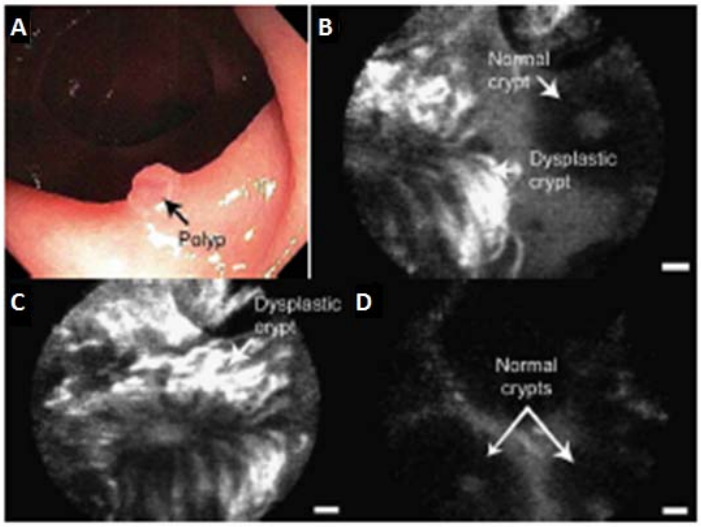

Figure 5. In vivo confocal fluorescence images of the border between colonic adenoma and normal mucosa, showing peptide binding to dysplastic epithelial cells. The endoscopic view (A), border (B), dysplastic crypt (C) and adjacent mucosa (D) are shown with scale bars of 20µm. (Hsiung PL, Hardy J, Friedland S, *et al*. Detection of colonic dysplasia *in vivo* using a targeted heptapeptide and confocal microendoscopy. Nat Med 2008;14:454-8; with permission)

Interferometric Techniques

Various interferometric techniques have been developed to yield morphological information about the tissue. The light scattered from tissue can be interfered with a reference beam, providing information about the structure of the tissue. Illumination with a source characterized by a low coherence length, a technique known as time domain low coherence interferometry (LCI), can be used to selectively process light scattered from varying depths in the tissue by changing the distance travelled by the reference arm [41,42]. By sweeping the wavelength of the light source, rather than modifying the distance travelled by the reference beam, Frequency Domain LCI demonstrates further improvements in SNR and an increase in data acquisition time [41,43,44]. Furthermore, the angle at which the light is incident on the tissue can be varied using a technique called angle resolved LCI (a/LCI), yielding information about the angular intensity distribution of the scattered light as a function of depth [45-47]. The detected light can then be processed to yield information about the mean size and relative refractive index of cell nuclei in the tissue.

Optical coherence tomography (OCT) is an imaging interferometric technique that obtains multiple LCI scans, yielding 3-D images with micrometer resolution that provide detailed morphologic information about the tissue. While OCT has become a clinical resource in ophthalmology, endoscopic OCT has been demonstrated *in vivo* in the GI tract to provide high resolution images of the esophagus [48]. Recent work has investigated combining the biochemical information gained from molecular imaging with the high resolution images obtained from interferometric techniques like OCT. Yuan *et al* combined fluorescence molecular imaging (FMI) with OCT using a dichroic to simultaneously illuminate the tissue with a different wavelength for each modality [49]. Excised small and large bowels (N=4) of male C57BL/6J *APCMin*/+ mice were imaged, and fluorescence was obtained using UEA-1 conjugated contrast agent, which has been shown to bind to the surfaces of adenomatous polyps due to the over expression of the carbohydrate α-L-fucose on the surface of the polyps. Backscattered and fluorescent light were captured allowing the scattering coefficient and fluorescence intensity of the tissue to be measured simultaneously. In Figure 6A, an OCT image where the tissue surface height is color coded reveals four hot spots, indicating the presence of four raised polyps. Cross sectional OCT images and histology for the lines in Figure 6A are displayed in Figures 6B-6E and 6F-6I, respectively. The raised polyps are easily distinguished from the surrounding tissue. The tissue scattering coefficient and fluorescence image are displayed in Figure 6J and 6K, and are fused in Figure 6L, showing that the polyps exhibit higher scattering coefficients and fluorescence intensities than the surrounding tissue.

In other work, Iftimia *et al.* demonstrated co-registered ex vivo widefield fluorescence imaging and OCT using colon tissue from *ApcMin* mice [50]. Fluorescence imaging was achieved using poly(epsilon-caprolactone) microparticles labeled with a NIR dye and

functionalized with an RGD (argenine-glycine-aspartic acid) peptide to recognize the over expression of αvβ3 integrin receptor (ABIR). Winkler *et al.* combined OCT and fluorescence microscopy *in vivo* via endoscope using the azoxymethane-treated mouse model of colon cancer [51]. Fluorescence was achieved using the conjugation of a near-infrared fluorescent dye, Cy5.5, to single chain vascular endothelial growth factor. The combination of OCT and spectroscopy has also been investigated by Robles *et al*., who demonstrated the combination of both techniques using a source in the visible domain [52].

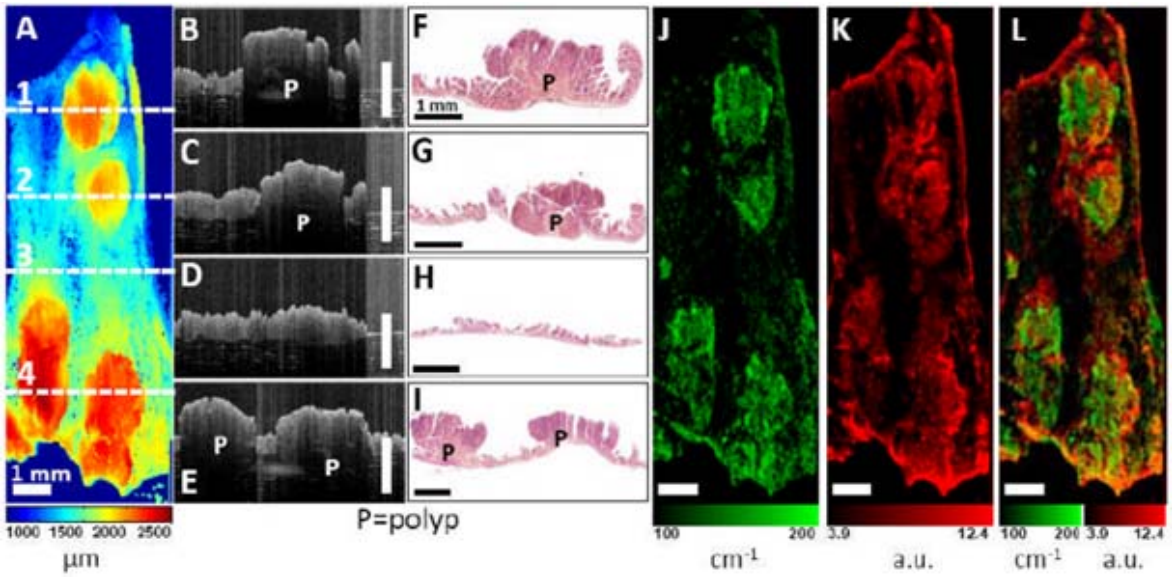

Figure 6. Co-registered OCT/FMI imaging of intestinal polyps incubated with UEA-1 conjugated liposomes *ex vivo*. (A) OCT *en face* surface image. Tissue surface height is color-coded (ranging from 1 – 2.5 mm). Four polyps are clearly visible as elevated tissue surface height. (B-I) Cross-sectional OCT images corresponding to the horizontal lines 1-4 in A. Polyps (P) are visible as protruded masses in B, D, and H. Normal mucosa is shown in F. The scale bars in B-H are physical distance and a refractive index of 1.4 for tissue was used for calculating the physical distance. Corresponding histology (C, E, G, I) confirm the OCT images. (J) Tissue scattering coefficient (μ_s) image ranges from 100-200 cm^{-1}. Polyps show higher extinction coefficients. (K) Fluorescence image using the UEA-1 conjugated contrast agents. Fluorescence intensities are higher around polyp areas than the surrounding mucosa. (L) Fused scattering coefficient and fluorescence image with a scale bar of 1 mm. (Yuan S, Roney CA, Wierwille J, *et al*. Combining Optical Coherence Tomography with Fluorescence Molecular Imaging: Towards Simultaneous Morphology and Molecular Imaging. Phys Med Biol 2010;55:191–206; with permission.)

Conclusion

The need to improve the detection and classification of early stage neoplasia in the esophagus and colon has led to the development of a variety of widefield and high resolution optical imaging techniques. While some widefield techniques, such as AFI and NBI, do not require the application of contrast agents, these techniques and others could potentially be enhanced by the use of contrast agents that specifically highlight biochemical changes associated with neoplasia. Widefield fluorescence and high resolution imaging such as confocal laser endomicroscopy and OCT can combine molecular and morphological imaging to yield information about the structure and nature of the tissue. Of specific note are the recent advancements in targeted contrast agents, which have been used to highlight areas of dysplasia.

While promising, there are a number of challenges that must be solved before large scale implementation of optical molecular imaging can be achieved. First, larger scale, multi-central studies are required with appropriate histologic endpoints to properly assess the diagnostic potential of each modality. In cases where commercial instruments are not yet available, additional effort is required to ensure standardization of imaging platforms. In the longer term, further study is required to examine whether the use of new modalities has a positive impact on patient outcomes. There are additional barriers to the implementation of approaches that rely on targeted contrast agents, including the identification of biomarkers which are sufficiently and consistently upregulated in neoplasia, the development of appropriate delivery formulations, and navigation of complex regulatory barriers.

References

1. American Cancer Society, Global Cancer Facts & Figures 2nd Ed. Atlanta: American Cancer Society, 2008.

2. Ries L, Melbert D, Krapcho M, et al. SEER Cancer Statistics Review, 1975–2004. Bethesda, MD: National Cancer Institute; 2007.

3. Wang KK, Sampliner, RE. Updated Guidelines 2008 for the Diagnosis, Surveillance, and Therapy of Barrett's Esophagus. Am J Gastronterol 2008;103:788-97.

4. American Cancer Society. *Cancer Facts & Figures 2012*. Atlanta: American Cancer Society; 2012.

5. American Cancer Society. Colorectal Cancer Facts & Figures 2011-2013. Atlanta: American Cancer Society, 2008.

6. Kahi CJ, Imperiale TF, Juliar BE, *et al*. Effect of screening colonoscopy on colorectal cancer incidence and mortality. Clin Gastroenterol Hepatol 2009;7:770-5.

7 . Peter C. Enzinger, M.D., and Robert J. Mayer, M.D. Esophageal Cancer. N Engl J Med 2003;349:2241-52.

8. Vieth M, Ell C., Gossner L., *et al*. Histological Analysis of Endoscopic Resection Specimens From 326 Patients with Barrett's Esophagus and Early Neoplasia. Endoscopy 2004;36:776-81.

9. Sharma P, McQuaid K, Dent J, *et al*. A Critical Review of the Diagnosis and Management of Barrett's Esophagus: The AGA Chicago Workshop. Gastroenterol 2004;127:310-330.

10. Reid BJ, Petras R, Gramlich TL, *et al*. The diagnosis of low-grade dysplasia in Barrett's esophagus and its implicatinos for disease progression. Am J Gastroenterol 2000;95:3383-87.

11. Goetz M and Kiesslich R. Advanced imaging of the gastrointestinal tract: research vs. clinical tools? Curr Opin Gastroenterol 2009;25:412-21.

12. Singh R, Mei SC, Sethi S. Advanced endoscopic imaging in Barrett's oesophagus: a review on current practice. World J Gastroenterol 2011;17;4271-6.

13. Singh R, Karageorgiou H, Owen V, *et al*. Comparison of high-resolution magnification narrow-band imaging and White-light endoscopy in the prediction of histology in Barrett's oesophagus. Scan J Gastroenterol 2009;44:85-92.

14. Muto M, Minashi K, Yano T, *et al*. Early detection of superficial squamous cell carcinoma in the head and neck region and esophagus by narrow band imaging: a multicenter randomized controlled trial. J Clin Oncol 2010;28:1566-72.

15. Jayasekera C, Taylor ACF, Desmond PV, *et al*. Added value of narrow band imaging and confocal laser endomicroscopy in detecting Barrett's esophagus neoplasia. Endoscopy 2012;44:1089-95.

16. Sharma P, Hawes RH, Bansal A, *et al*. Standard endoscopy with random biopsies versus narrow band imaging targeted biopsies in Barrett's oesophagus: a prospective, international, randomized controlled trial. Gut 2011;62:15-21.

17. Pasha SF, Leighton JA, Das A, *et al*. Comparison of the yield and miss rate of narrow band imaging and white light endoscopy in patients undergoing screening or surveillance colonoscopy: a meta-analysis. Am J Gastroenterol 2012;107:363-70.

18. Monici M. Cell and tissue autofluorescence research and diagnostic applications. Biotech Ann Rev 2005;11;227-56.

19. Kara MA, Peters FP, Fockens P, *et al*. Endoscopic video-autofluorescence imaging followed by narrow band imaging for detecting early neoplasia in Barrett's esophagus. Gastrointest Endosc 2006;64:176-85.

20. Kara MA, Peters FP, Ten Kate FJ, *et al*. Endoscopic video autofluorescence imaging may improve the detection of early neoplasia in patients with Barrett's esophagus. Gastrointest Endosc. 2005;61:679-85.

21. Thekkek N, Anandasabapathy S, and Richards-Kortum R. Optical molecular imaging for detection of Barrett's-associated neoplasia. World J Gastroenterol.2011; 17: 53–62.

22. Curvers WL, Singh R, Song LM, *et al*. Endoscopic tri-modal imaging for detection of early neoplasia in Barrett's oesophagus: a multi-centre feasibility study using high-resolution endoscopy, autofluorescence imaging and narrow band imaging incorporated in one endoscopy system. Gut 2008; 57;167–72.

23. Curvers W, van Vilsteren FG, Baak LC, *et al*. Endoscopic trimodal imaging versus standard video endoscopy for detection of early Barrett's neoplasia: a multicenter randomized, crossover study in general practice. Gastrointest Endosc 2011;73:195-203.

24. Ishimura N, Amano Y, Uno G, *et al*. Endoscopic characteristics of short-segment Barrett's esophagus, focusing on squamous islands and mucosal folds. J Gastroenterol Hepatol 2012;27:82-7.

25. Shahid MW, Buchner AM, Coron E, *et al*. Diagnostic accuracy of probe-based confocal laser endomicroscopy in detecting residual colorectal neoplasia after EMR: a prospective study. Gastrointest Endosc 2012;75:525-33.

26. Sharma P, Meining AR, Coron E, *et al*. Real-time increased detection of neoplastic tissue in Barrett's esophagus with probe-based confocal laser endomicroscopy: final results of an international multicenter, prospective, randomized, controlled trial. Gastrointest Endosc 2011;74:465-72.

27. Wallace MB, Sharma P, Lightdale C, *et al*. Preliminary accuracy and interobserver agreement for the detection of intraepithelial neoplasia in Barrett's esophagus with probe-based confocal laser endomicroscopy. Gastrointest Endosc 2010;72:19-24.

28. Dunbar KB, Okolo P 3rd, Montgomery E, *et al*. Confocal laser endomicroscopy in Barrett's esophagus and endoscopically inapparent Barrett's neoplasia: a prospective, randomized, double-blind, controlled, crossover trial. Gastrointest Endosc 2009; 70:645-54.

29. Goetz M, Ziebart A, Foersch S, *et al*. *In vivo* molecular imaging of colorectal cancer with confocal endomicroscopy by targeting epidermal growth factor receptor. Gastroenterology 2010;138:435-46

30. Gaddam S, Mathur SC, Singh M, *et al.* Novel Probe-Based Confocal Laser Endomicroscopy Criteria and Interobserver Agreement for the Detection of Dysplasia in Barrett's Esophagus. Am J Gastroenterol 2011; 106:1961–9.

31. Wang T, Friedland S, Sahbaie P, *et al*. Functional Imaging of Colonic Mucosa with a Fibered Confocal Microscope for Real-Time *In Vivo* Pathology. Clin Gastroenterol Hepatol 2007;5:1300-5.

32. Shahid MW and Wallace MB. Endoscopic Imaging for the Detection of Esophageal Dysplasia and Carcinoma. Gastrointest Endosc Clin N Am 2010;20:11-24.

33. Wang KK, Prasad G, Tian J. Endoscopic mucosal resection and endoscopic submucosal dissection in esophageal and gastric cancers. Curr Opin Gastroenterol 2010;26:453-8.

34. Muldoon TJ, Anandasabapathy S, Maru D, *et al*. High-resolution imaging in Barrett's esophagus: a novel, low-cost endoscopic microscope. Gastrointest Endosc 2008;68:737-44.

35. Muldoon TJ, Pierce MC, Nida DL, *et al*. Subcellular-resolution molecular imaging within living tissue by fiber microendoscopy. Opt Express 2007;15:16413-23.

36. Bird-Lieberman EL, Neves AA, Lao-Sirieix P, *et al*. Molecular imaging using fluorescent lectins permits rapid endoscopic identification of dysplasia in Barrett's esophagus. Nat Med 2012;18:315-21.

37. Miller SJ., Lee CM, Joshi BP, *et al*. Targeted detection of murine colonic dysplasia *in vivo* with flexible multispectral scanning fiber endoscopy. J Biomed Opt. 2012;17.

38. Bedard N, Quang T, Schmeler K, *et al*. Real-time video mosaicing with a high-resolution microendoscope. Biomed Opt Express 2012;3:2428–35.

39. Behrens A, Bommes M, Stehle T, *et al*. Real-time image composition of bladder mosaics in fluorescence endoscopy. Computer Science - Research and Development, 2011;26:51-64.

40. Hsiung PL, Hardy J, Friedland S, *et al*. Detection of colonic dysplasia *in vivo* using a targeted heptapeptide and confocal microendoscopy. Nat Med 2008;14:454-8.

41. Drexler W, Fujimoto J. Optical Coherence Tomography: Technology and Applications. Springer 2008.

42. C. H. Yang, L. T. Perelman, A. Wax, *et al.* Feasibility of field-based light scattering spectroscopy. J. Biomed. Opt. 5, 138 (2000).

43. Wax A, Yang C, Izatt JA. Fourier-domain low-coherence interferometry for light-scattering spectroscopy. Opt Lett 2003;28:1230-2.

44. Graf RN, Wax A. Nuclear morphology measurements using Fourier domain low coherence interferometry. Opt Exp 2005;13:4693-8.

45. Terry NG, Zhu Y, Rinehart MT, *et al*. Detection of dysplasia in Barrett's esophagus with *in vivo* depth resolved nuclear morphology measurements. Gastroenterology 2011; 140:42–50.

46. Zhu Y, Terry NG, and Wax A. Development of angle resolved low coherence interferometry for clinical detection of dysplasia. J Carcinog 2011;10:1-9.

47. Brown WJ, Pyhtila JW, Terry NG, et al. Review and Recent Development of Angle-Resolved Low-Coherence Interferometry for Detection of Precancerous Cells in Human Esophageal Epithelium. IEEE J Sel Top Quant Elec 2008;14:88-97.

48. Zhou C, Tsai TH, Lee HC, *et al*. Characterization of buried glands before and after radiofrequency ablation by using 3-dimensional optical coherence tomography. Gastrointest Endosc 2012;76: 32–40.

49. Yuan S, Roney CA, Wierwille J, *et al*. Combining Optical Coherence Tomography with Fluorescence Molecular Imaging: Towards Simultaneous Morphology and Molecular Imaging. Phys Med Biol 2010;55:191–206.

50. Iftimia N, Iyer AK, Hammer DX, *et al*. Fluorescence-guided optical coherence tomography imaging for colon cancer screening: a preliminary mouse study. Biomed Opt Express 2012;3:178–91.

51. Winkler AM, Rice PF, Weichsel J, *et al*. *In Vivo*, Dual-Modality OCT/LIF Imaging Using a Novel VEGF Receptor-Targeted NIR Fluorescent Probe in the AOM-Treated Mouse Model. Mol Imaging Biol. 2011;13:1173-82.

52. Robles FE, Wilson C, Grant G, *et al*. Molecular imaging true-colour spectroscopic optical coherence tomography. Nat Phot 2011;5:744-7.